



ELSEVIER

Available online at www.sciencedirect.com

SCIENCE @ DIRECT®

Journal of Magnetism and Magnetic Materials 295 (2005) 257–262



www.elsevier.com/locate/jmmm

Textured Co nanowire arrays with controlled magnetization direction

H.N. Hu^{a,*}, H.Y. Chen^a, S.Y. Yu^a, J.L. Chen^a, G.H. Wu^a, F.B. Meng^b, J.P. Qu^b,
Y.X. Li^b, H. Zhu^c, John Q. Xiao^c

^a*Beijing National Laboratory for Condensed Matter Physics, State Key Laboratory for Magnetism, Institute of Physics, Chinese Academy of Sciences, Beijing 100080, China*

^b*School of Material Sciences and Engineering, Hebei University of Technology, Tianjin 300130, People's Republic of China*

^c*Department of Physics and Astronomy, University of Delaware, Newark, DE 19716, USA*

Received 11 November 2004; received in revised form 21 December 2004

Available online 5 February 2005

Abstract

Textured HCP Co nanowires with preferentially oriented (100) along the growth direction were fabricated by electrodeposition at high potential. Further increase of deposition potential results in the formation of twist wires with circumferential strain. These conclusions are unambiguously reached by combining TEM, XRD rocking curves and pole figures. The magnetic properties are determined by the combination of magnetocrystalline, shape, and stress anisotropies and magnetostatic interaction. Consequently, the magnetic easy axis can be tuned with structure and temperature, thus paving the road for magnetic nanowire array use in applications where self-biasing of magnetization is necessary.

© 2005 Elsevier B.V. All rights reserved.

PACS: 75.75; 81.07; 81.07.B

Keywords: Nanowire electrodeposition texture; Porous anodic aluminum oxide

1. Introduction

One-dimensional nanostructures are of great interest because of potential applications in areas such as high-density perpendicular magnetic re-

coding media and nanosensors [1–3]. More recently, exciting developments in magnetic domain switching by spin-polarized currents seem to promise breakthroughs in magnetic memory technology [4,5]. A spin-polarized current of a high current density can be easily achieved in one-dimensional structure. Precise structural control of these one-dimensional structures allows us to understand the mechanism of current-driven spin

*Corresponding author. Tel.: +86 1 082 649 247;

fax: +86 1 082 649 485.

E-mail address: hnhu@aphy.iphy.ac.cn (H.N. Hu).

dynamics. The synthesis and precise control of such a magnetic nanostructure on a large scale is a challenging issue in materials science. One strategy is to electrodeposit magnetic nanowires into nanochannels of porous anodic aluminum oxide (AAO) templates, which have been utilized by many groups to prepare magnetic metals including Ni, Co, and Fe [1–3,6–13]. In the case of Co nanowires, almost all electrodeposited Co nanowires are polycrystalline. In this letter we report the preparation of (100) oriented Co nanowires with hexagon close packed (HCP) structure in a controllable fashion. The structure has been verified with conventional X-ray diffraction (XRD), scanning electron microscopy (SEM) and transmission electron microscopy (TEM). Detailed X-ray rocking curve and pole figure measurements reveal the formation of twisted HCP structure by controlling the fabrication parameters. The circumferential tension in twisted HCP structures significantly influences the magnetic anisotropy and can be used to control the magnetization direction in Co nanowire array.

2. Experiment procedure

Porous anodic aluminum oxide (AAO) template was prepared by a two-step anodizing process on aluminum foils [14,15]. Al foil with purity of 99.999% was anodized in 0.3 M under a constant voltage of 40 V at 12 °C. After anodization, the remaining aluminium substrate and its barrier layer at the bottom of the AAO template were removed to obtain the through holes AAO template with pore length of 40 μm and uniform diameters of 60 nm. A Cu layer was sputter deposited on one side of the AAO template to serve as the working electrode in a two-electrode electrochemical cell. An aqueous bath (pH \sim 3.0) containing 0.2 M Co^{2+} and H_3BO_3 (30 g/l) was used to prepare Co nanowire at room temperature with constant potential of -2 V or higher. Co-1 and Co-2 samples were deposited from the same electrolyte with potential of -1.95 and -2.15 V, respectively. SEM and TEM were used to characterize the morphology and the structure of the nanowires. The X-ray rocking curve and pole

figure measurements were carried out in a Philips X'Pert MPD instrument using the Cu $\text{K}\alpha$ radiation. The magnetic measurements were performed using a superconducting quantum interference device (SQUID) magnetometer.

3. Results and discussion

Fig. 1 shows the SEM and TEM results on the Co nanowire arrays and an isolated nanowire. The length of Co nanowires is about 40 μm , consistent with AAO template thickness. The wires show uniform diameter of about 60 nm, resulting in a high aspect ratio of about 700. Selected-area electron diffraction (SAED) pattern has been performed on different Co nanowires and different positions on individual wires. All

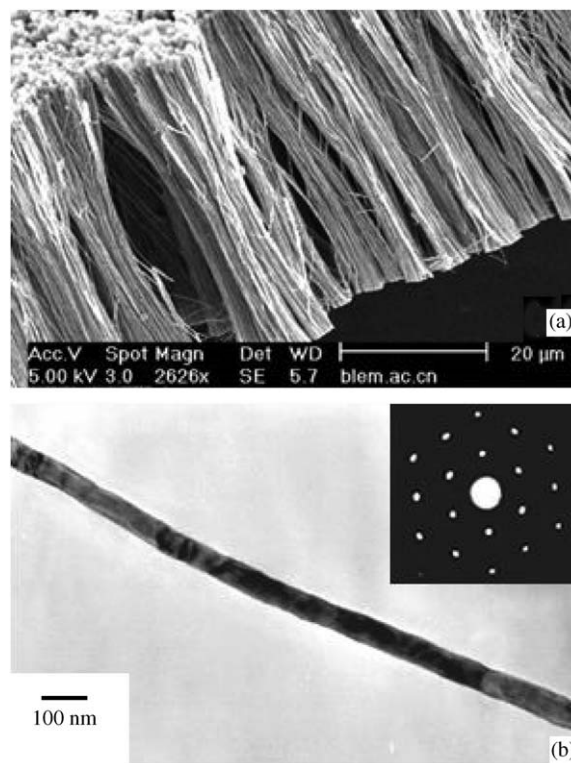


Fig. 1. (a) SEM images of cross-section view of Co nanowire arrays after removing the AAO template; (b) typical bright field TEM image of a single-crystal Co nanowire and electron diffraction from the same sample (inset) showing the HCP structure with c -axis aligned perpendicular to the wire.

obtained diffraction patterns show hexagonal symmetry (inset in Fig. 1b), indicating that wires are single crystal HCP structure with c -axis perpendicular to the wire.

Fig. 2 shows XRD spectra of Co nanowire arrays embedded in templates. All samples show only a sharp (100) peak of HCP Co, indicating the preferential orientation of whole single-crystalline wires. The inset of Fig. 2 shows the results from X-ray rocking curve of (100) reflection. Most of samples, denoted as Co-1, show one sharp peak centered at the specular angle of 20.8° with narrow peak widths at half-maximum (FWHM) in the range of 2.38 – 5.51° . Assuming a Gaussian distribution, these results indicate that at least 75% of the wires have a preferential orientation within 1.2 – 2.8° of the [100] direction. Similar analyses for polycrystalline samples show a larger distribution angle up to 9° [8]. Samples electrodeposited at the potential of -2.15 V (denoted as Co-2) show very different rocking curves, indicated in the inset of Fig. 2. Although they have the same sharp (100) XRD peak as Co-1 samples, there is no peak at 20.8° in rocking curves. Interestingly, there are two twin-peaks with the same intensity at 15.7° and 26.1° , respectively (i.e., about $\pm 5^\circ$ mirror imaging the [100] characteristic angle of 20.8°).

Combining the results from SEM, TEM, XRD and X-ray rocking curves, we can conclude that

each individual nanowire is single crystal and has [100] preferred orientation along the wires. The nanowires array has random c -axis distribution in the AAO template plane. The sharp (100) peak in XRD and the narrow FWHM of rocking curves of 2.38° indicates the excellent pore parallelity in AAO templates as well as a near-perfect texture in our nanowire arrays. This clearly indicates that optimum deposition condition can be achieved to fabricate well-textured nanowires array over a large area. It is important to emphasize that the unusual twin-peak in rocking curves of Co-2 samples cannot be explained by the parallelity deviation in pore structure, nor can it be explained with the deviation from the overall orientation. A poor parallelity only increases the FWHM of the rocking curves, and orientation deviation increases the FWHM and shifts the peak position.

To explain the double peaks in rocking curves for Co-2 samples, we performed pole figure measurement and (100) and (101) pole figures for Co-1 and Co-2 samples as shown in Fig. 3. The tilt angle (α) was varied from 0 – 85° in steps of 5° . The azimuth angle (β) was varied from 0 – 355° in steps of 5° . Fig. 3(a) shows a well-defined HCP (100) sharp peak at $\alpha = 0^\circ$ for Co-1, further confirming the high degree of (100) alignment of

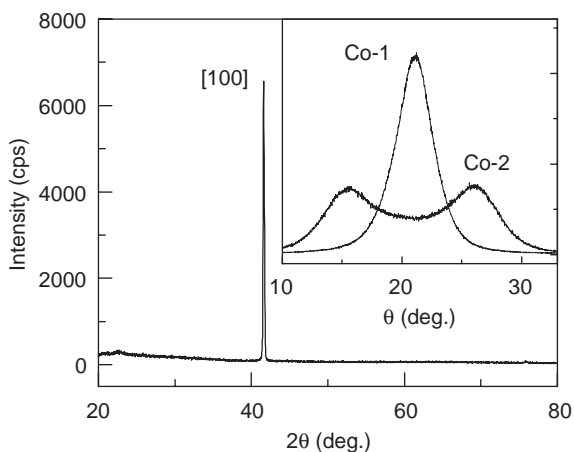


Fig. 2. X-ray diffraction (XRD) spectrum of Co nanowire arrays embedded in porous alumina template. Inset is the (100) rocking curve for two types of nanowire arrays.

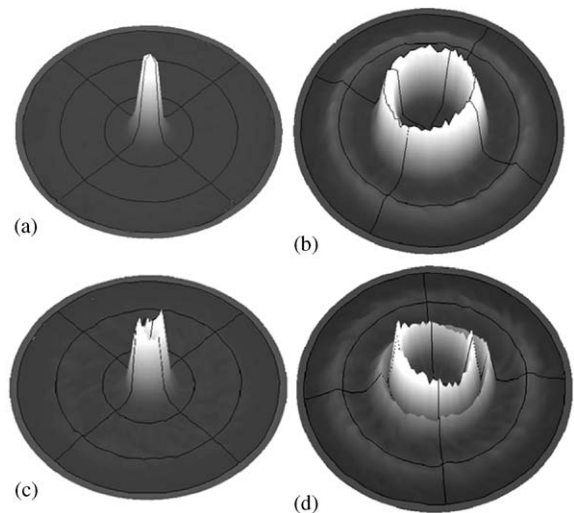


Fig. 3. Three-dimensional (100) (a) and (101) (b) pole figures of Co-1 samples and three-dimensional (100) (c) and (101) (d) pole figures of Co-2 samples, respectively.

nanowires along the wire direction in Co-1 samples. The HCP (101) peak in Fig. 3(b) shows the diffraction maximum as a crateriform ring located at $\alpha = 30^\circ$, corresponding to the angle between the neighboring [100] and [101] planes. This means that the $\langle 101 \rangle$ axis of nanowires are randomly distributed in the array. Based on this observation, one may easily conclude that the c -axis of single-crystalline wires also distribute randomly in the array plane.

For Co-2 samples, the (100) peak has a volcano shape located at about $\alpha = 5^\circ$ surrounding the center of the pole figure (Fig. 3c). Its (101) pole figure shows two crateriform rings located at about $\alpha = 25^\circ$ and 35° , respectively. These shifted angles are consistent with twin-peak pattern observed in (100) rocking curve (inset of Fig. 2). If twin peak pattern in rocking curve suggests lattice structure shown in Fig. 4d, then the pole figure suggests that such distortion have circular symmetry. Here, we propose a model of twisted wire shown in Fig. 4 which will result in this cone structure, this model is also consistent with observed magnetic properties to be discussed later.

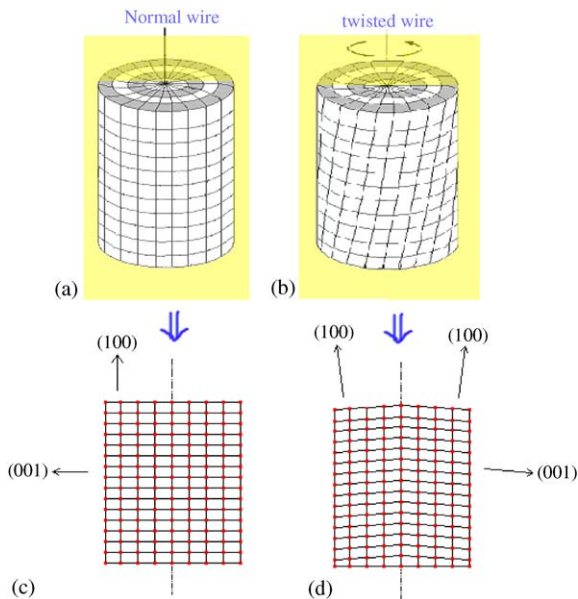


Fig. 4. The twisted nanowire model. The cross-section of both normal and twisted nanowires are shown below the three-dimensional diagram. (100) and (001) orientations are labeled in the figure. (See text for detailed explanation).

If the wire is twisted as it grows (Fig. 4b), the atoms on the second plane will not be directly above these on the first plane, but shifted along the twisted direction. Consequently, the distance between the first and second planes is reduced. The reduction is most on the outmost radius and zero along the center line since the twist creates the largest displacement at the outmost radius. It is clear the formation of this structure must be accompanied by dislocations or defects. The cross-sectional view of such a distortion is shown in Fig. 4d. The angle between wire axis and (100) orientation for the twisted wire, in our case, should be about 5° . This effect gives rise to the twin peaks shown in the inset of Fig. 2, and in the pole figure volcano-like (100) peak at $\alpha = \pm 5^\circ$ in Fig. 3c. Similar analysis shows that double crateriform rings should be observed for (101) orientation located at $\alpha = 30 \pm 5^\circ$. Experimental pole figure of (101) for twisted nanowire array is shown in Fig. 3d. This is the only structure that explains consistently the results shown in the rocking curves and pole figures. This model has never been proposed before, since no pole figure studies have been done in nanowire array.

Magnetic properties were measured by a SQUID magnetometer from 5 to 300 K. Fig. 5 shows the hysteresis loops of Co-1 (a, b), Co-2 (c, d), and Co-2 with template partially etched away (e, f) at 5 and 300 K, respectively. The

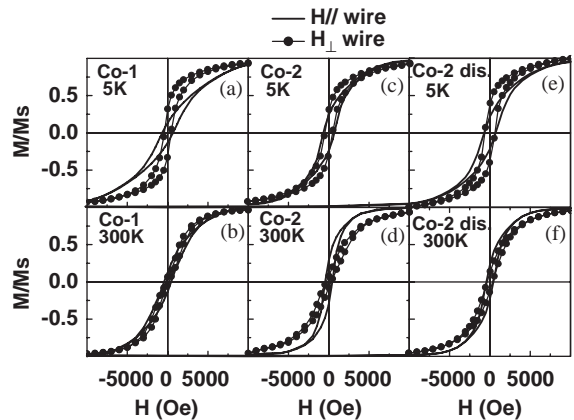


Fig. 5. Hysteresis loops of sample Co-1 (a, b), Co-2 (c, d) and Co-2 with template partially etched away (e, f). Field is applied perpendicular (---) or parallel (—) to the nanowires.

control of anisotropy by structure and temperature is clear: for untwisted Co-1 wire array, the easy axis is perpendicular to the wires at low temperature and gradually decreases with increasing temperatures, while twisted Co-2 wire array shows an easy axis along the wires at high temperatures and decreases with decreasing temperatures. The total anisotropy represents the competition among magnetocrystalline, shape, and stress anisotropies and dipolar interaction [7,9]. For HCP Co, the magnetocrystalline anisotropy creates an easy magnetization direction along the *c*-axis, which is reduced due to the random *c*-axis orientations in both Co-1 and Co-2 samples. The dipolar interaction, which is the same for both samples because of the same diameter and length, leads to an easy magnetization direction perpendicular to the nanowire array. If the stress effect in the Co-1 samples is neglected, then the sum of magnetocrystalline anisotropy and dipolar interaction is larger than the shape anisotropy. This results in an easy magnetization direction perpendicular to the nanowires. The magnetocrystalline anisotropy decreases faster than shape anisotropy and dipolar interaction with increasing temperature, leading to the temperature-dependent behaviors observed in sample Co-1. In sample Co-2, in addition to crystalline and shape anisotropies and dipolar interaction, there is a stress anisotropy, $E_{me} = \frac{3}{2}\lambda\sigma\sin^2\theta$, where λ is the magnetostriction coefficient, σ the stress, and θ the angle between M_s and σ . In Co-2, the positive circumferential tensile stress σ and negative λ for Co along the *c*-axis gives rise to a negative stress anisotropy, implying that along the wire direction is an easy axis [16]. At low temperature, the stress and shape anisotropy balances the magnetocrystalline anisotropy and dipolar interaction, resulting in similar magnetic properties in two directions. For the same reason as in Co-1, at the room temperature, the magnetization prefers to be along the wire direction. It should be noted that the coercivity of Co-2 samples is always larger than that of Co-1 samples because of this additional stress anisotropy. To confirm the stress anisotropy in Co-2 sample, the Al₂O₃ template was partially removed to release portion of stress, and the magnetic properties at 5 and 300 K are shown

in Fig. 4(e,f). As anticipated the hysteresis loops are between those non-stressed Co-1 nanowire arrays and stressed (twisted) Co-2 nanowire array (Co-2), clearly demonstrating that the stress anisotropy plays a crucial role here.

4. Conclusions

Textured Co nanowire with preferred growth orientation of (100) has been fabricated by electrodeposition at high potential. Further increase of deposition potential results in the formation of twist wires. These conclusions are unambiguously reached by combining TEM, XRD rocking curve and pole figure measurements. The magnetic properties are determined by the combination of magnetocrystalline, shape, and strain anisotropies and dipolar interaction. Consequently, the magnetic easy axis can be tuned with structure and temperature, thus paving the road for magnetic nanowire array use in applications where self-biasing of magnetization is necessary.

Acknowledgements

This work was supported by National Natural Science Foundation of China Grant no. 50371101. JQX would also like to acknowledge the support from Grant AFOSR F49620-03-1-0351 and American Chemical Society Petroleum 40057-AC5M.

References

- [1] T.M. Whitney, J.S. Jiang, P.C. Searson, C.L. Chien, *Science* 261 (1993) 1316.
- [2] D. Almalawi, N. Coombs, M. Moskovits, *J. Appl. Phys.* 70 (1991) 4421.
- [3] T. Thurn-Albrecht, J. Schotter, G.A. Kastle, N. Emley, T. Shibauchi, L. Krusin-Elbaum, K. Guarini, C.T. Black, M.T. Tuominen, T.P. Russell, *Science* 290 (2000) 2126.
- [4] M. Klaui, C.A.F. Vaz, J.A.C. Bland, W. Wernsdorfer, G. Faini, E. Cambril, L.J. Heyderman, *APL* 83 (2003) 105.
- [5] T.Y. Chen, Y. Ji, C.L. Chien, *APL* 84 (2004) 380.
- [6] P.M. Paulus, F. Luis, M. KroK II, G. Schmid, L.J. de Jong, *J. Magn. Magn. Mater.* 224 (2001) 180.
- [7] R. Ferre', K. Ounadjela, J.M. George, L. Piroux, S. Dubois, *Phys. Rev. B* 56 (1997) 14066.

- [8] J.-L. Maurice, D. Imhoff, P. Etienne, O. Durand, S. Dubois, L. Piraux, J.-M. George, P. Galtier, A. Fert, *J. Magn. Magn. Mater.* 184 (1998) 1.
- [9] K. Ounadjela, R. Ferre', L. Louail, J.M. George, J.L. Maurice, L. Piraux, S. Dubois, *J. Appl. Phys.* 81 (1997) 5455.
- [10] H. Zeng, R. Skomski, L. Menon, Y. Liu, S. Bandyopadhyay, D.J. Sellmyer, *Phys. Rev. B* 65 (2002) 134426.
- [11] Shihui Ge, Xiao Ma, Chao Li, Wei Li, *J. Magn. Magn. Mater.* 226–230 (2001) 1867.
- [12] L. Piraux, S. Dubois, J.L. Duvai, K. Ounadjela, A. Fert, *J. Magn. Magn. Mater.* 175 (1997) 127.
- [13] Y. Henry, K. Ounadjela, L. Piraux, S. Dubois, J.-M. George, J.-L. Duvail, *Eur. Phys. J. B* 20 (2001) 35.
- [14] H. Masuda, K. Fukuda, *Science* 268 (1995) 1466.
- [15] Y.W. Wang, L.D. Zhang, G.W. Meng, X.S. Peng, Y.X. Jin, J. Zhang, *J. Phys. Chem. B* 106 (2002) 2502.
- [16] B.D. Cullity, *Introduction to Magnetic Materials*, Addison-Wesley, MA, 1972, pp. 260–264.